arXiv:1002.0946v1 [cond-mat.mes-hall] 4 Feb 2010

Quantized Anomalous Hall Effect in Magnetic Topological Insulators

Rui Yu,[1] Wei Zhang,[1] Hai-Jun Zhang,[1,2] Shou-Cheng Zhang,[2,3]

Xi Dai,[1*] Zhong Fang[1*]

[1]*Beijing National Laboratory for Condensed Matter Physics and Institute of Physics, Chinese Academy of Sciences, Beijing 100190, China,*

[2]*Department of Physics, McCullough Building, Stanford University Stanford, CA 94305-4045,*

[3] *Center for Advanced Study, Tsinghua University, Beijing 100084, China*

(Dated: February 4, 2010)

Abstract

The Hall effect, the anomalous Hall effect and the spin Hall effect are fundamental transport processes in solids arising from the Lorentz force and the spin-orbit coupling respectively. The quantum versions of the Hall effect and the spin Hall effect have been discovered in recent years. However, the quantized anomalous Hall (QAH) effect has not yet been realized experimentally. In a QAH insulator, spontaneous magnetic moments and spin-orbit coupling combine to give rise to a topologically non-trivial electronic structure, leading to the quantized Hall effect without any external magnetic field. In this work, based on state-of-art first principles calculations, we predict that the tetradymite semiconductors Bi_2Te_3, Bi_2Se_3, and Sb_2Te_3 form magnetically ordered insulators when doped with transition metal elements (Cr or Fe), in sharp contrast to conventional dilute magnetic semiconductor where free carriers are necessary to mediate the magnetic coupling. Magnetic order in two-dimensional thin films gives rise to a topological electronic structure characterized by a finite Chern number, with quantized Hall conductance e^2/h. Experimental realization of the long sought-after QAH insulator state could enable robust dissipationless charge transport at room temperature.

I. INTRODUCTION

Soon after the observation of the Hall effect, Hall also observed the anomalous Hall effect (AHE)[1,2] in ferromagnetic metals, where the Hall resistance arises from the spin-orbit coupling (SOC) between electric current and magnetic moments, even in the absence of external magnetic field. Recent progress on the mechanism of AHE have established a link between the AHE and the topological nature of Hall current due to SOC by adopting the Berry-phase concepts[3–6], in close analogy to the intrinsic spin Hall effect[8,9]. Given the experimental discovery of the quantum Hall[7] and quantum spin Hall (QSH) effects[10,11], it is natural to ask whether the AHE can also be quantized in a topological magnetic insulator, without the external magnetic field and the associated Landau levels.

A simple mechanism for the QAH insulator has been proposed in a two-band model of a two dimensional (2D) magnetic insulator[12]. In the limit of vanishing spin-orbit coupling, and large enough exchange splitting, the majority spin band is completely filled and minority spin band is empty. When the exchange splitting is reduced, the two bands intersect each other, leading to a band inversion, say near the Γ point. The degeneracy at the interaction region can be removed by turning on the SOC, giving rise to an insulator state with a topologically non-trivial band structure characterized by a finite Chern number and chiral edge states characteristic of the QAH state (see figures (1) and (2) of Ref.[12]). In alternative mechanisms of realizing the quantum Hall state without an external magnetic field, bond currents on a honeycomb lattice has been proposed[13], and the localization of the band electron could also give rise to a quantized plateau[14]. However, these mechanisms seem harder to realize experimentally.

Therefore, the crucial ingredients for realizing an QAH state are: (1) a ferromagnetically ordered 2D insulator which breaks the time-reversal symmetry; (2) a band inversion transition with strong SOC. In comparison with the QSH state, which satisfies the second condition[10,11], the first condition of the ferromagnetic order in an insulating state is harder to realize. However, the QSH insulators are usually good starting candidates for finding QAH effect due to its proximity to the band inversion. Given the QSH effect in HgTe quantum wells[10,11] through a band inversion transition by varying the thickness of the quantum well, the magnetically doped HgMnTe has been proposed as a candidate for the QAH insulator[15]. Unfortunately, the Mn moments do not order spontaneously in HgMnTe, and an additional,

small Zeeman field is required for the magnetic alignment of the Mn moments.

Recently, tetradymite semiconductors Bi_2Te_3, Bi_2Se_3, and Sb_2Te_3 have been theoretically predicted and experimentally observed to be topological insulators with the bulk band gap as large as 0.3eV in Bi_2Se_3[16–18]. The electronic states close to the Fermi level are the bonding and anti-bonding p orbitals, and these states undergo a band inversion at the Γ point when the strength of the spin-orbit coupling is increased[16]. When the thickness is reduced, the three dimensional (3D) topological insulator crosses over to a 2D topological insulator in an oscillatory fashion, as a function of the thickness[19]. In this work, we predict that this family of compounds doped with proper transition metal elements (Cr or Fe) should give the QAH state, the long sought-after quantum Hall state without any external magnetic field. In sharp contrast to the ferromagnetic order in conventional dilute-magnetic-semiconductors (DMS), where free carriers are necessary to mediate the ferromagnetic couplings via the RKKY mechanism[20–23], the magnetic dopants in tetradymite compounds naturally order ferromagnetically, mediated by the large spin susceptibility (of the van Vleck type) of the host insulator state. Due to the proximity to the band inversion transition, the exchange splitting leads to a topologically non-trivial insulating band structure with a finite Chern number. The recent experimental progresses on this family of compounds have demonstrated that well-controlled layer-by-layer MBE thin film growth can be achieved[24–27], and various transition metal elements (such as Ti, V, Cr, Fe) can be substituted into the parent compounds with observable ferromagnetism even above 100K[28–30]. By quantitative first-principles calculations, we further show that such ferromagnetic QAH insulating state can be also reached with Tc as high as around 70K. We will start from simple physical pictures based on model analysis, and then conclude by quantitative first-principles calculations.

II. THE VAN-VLECK PARAMAGNETISM IN BI_2SE_3 FAMILY COMPOUNDS

We first discuss minimal requirements for the ferromagnetic insulator phase in a semiconductor system doped with dilute magnetic ions under the assumption that the magnetic exchange among local moments is mediated by the band electrons. The whole system can then be divided into two sub-systems describing the local moments and band electrons respectively, which are coupled by a magnetic exchange term. Therefore if we only consider

the spatially homogeneous phase, the total free energy of the system can thus be written as,

$$F_{total} = \frac{1}{2}\chi_L^{-1} M_L^2 + \frac{1}{2}\chi_e^{-1} M_e^2 - J_{ex} M_L M_e - (M_L + M_e)\, H$$

where $\chi_{L/e}$ is the spin susceptibility of the local moments/electrons, $M_{L/e}$ denotes the magnetization for the local moment and electron sub-system and J_{ex} is the magnetic exchange coupling between the local moments and electrons. The onset of the ferromagnetic phase can be determined when the minimization procedure of the above free energy gives a non-zero magnetization without the external magnetic field H, which leads to $J_{ex}^2 - \chi_L^{-1}\chi_e^{-1} > 0$, or equivalently $\chi_L > \frac{1}{J_{ex}^2 \chi_e}$. In the dilute limit, we can neglect the direct coupling among the local moments, and then the spin susceptibility of the local moment sub-system takes the Curie-Weiss form, $\chi_L = x\mu_J^2/(3k_B T)$, where x is the concentration of the magnetic ions and μ_J is the magnetic moment of a single magnetic ion. Therefore, in order to have non-zero FM transition temperature, the above criterion requires a sizable spin susceptibility of the electron sub-system χ_e. In most of the DMS systems, e.g. $(Ga_{1-x}Mn_x)As$, the electronic spin susceptibility is negligible for the insulator phase and finite carrier concentration is required to conduct the magnetic coupling among local moments. As we shall discuss below, unlike the situation in GaAs, sizable spin susceptibility even exists through the Van Vleck paramagnetism for the insulator Bi_2Se_3, providing a new mechanism for ordering the doped magnetic ions.

The non-zero paramagnetic spin susceptibility for a band insulator has been known as the Van-Vleck paramagnetism[31] for a long time. For temperature much less than the band gap, the spin susceptibility for a band insulator can be obtained by the second order perturbation on the ground state, which can be written as,

$$\chi_e^{zz} = \sum_{E_{nk}<\mu; E_{mk}>\mu} 4\mu_0 \mu_B^2 \frac{\langle nk|\, \hat{S}_z\, |mk\rangle \langle mk|\, \hat{S}_z\, |nk\rangle}{E_{mk} - E_{nk}}. \quad (1)$$

where μ_0 is the vacuum permeability and μ_B is the Bohr magneton. It is then quite obvious that the van-Vleck paramagnetism is caused by the mixing of the conduction and valence bands induced by the spin operator in the presence of SOC. Such a mechanism is absent in the GaAs system, because the gap in GaAs is between mostly s and p bands and the matrix element of $\hat{S}_z$ is nearly zero between conduction and valence bands. In the case of Bi_2Se_3 family, the situation is completely different: both the conduction and valence bands are formed by the bonding and anti-bonding p orbitals and the energy gap is opened by the

spin-orbital coupling with band inversion, therefore the matrix element of the spin operator can be very large.

The Van-Vleck paramagnetism in Bi_2Se_3 family can be well understood using the following effective $k \cdot p$ Hamiltonian derived in ref.[16],

$$H_{3D}(\mathbf{k}) = \begin{bmatrix} \mathcal{M}(\mathbf{k}) & A_{xy}k_- & 0 & A_z k_z \\ A_{xy}k_+ & -\mathcal{M}(\mathbf{k}) & A_z k_z & 0 \\ 0 & A_z k_z & \mathcal{M}(\mathbf{k}) & -A_{xy}k_+ \\ A_z k_z & 0 & -A_{xy}k_- & -\mathcal{M}(\mathbf{k}) \end{bmatrix} + \epsilon_0(\mathbf{k}) \tag{2}$$

with $k_\pm = k_x \pm i k_y$, $\epsilon_0(\mathbf{k}) = C + D_{xy}\left(k_x^2 + k_y^2\right) + D_z k_z^2$, $\mathcal{M}(\mathbf{k}) = M_0 + B_{xy}\left(k_x^2 + k_y^2\right) + B_z k_z^{232}$, in the basis of $|P_z^+, \uparrow\rangle$, $|P_z^-, \downarrow\rangle$, $|P_z^+, \downarrow\rangle$, $|P_z^-, \uparrow\rangle$. The $\pm$ in the basis denote the even and odd parity states and $\downarrow\uparrow$ indicate the spin. As discussed before in Ref. [16], the four low energy states originate from the bonding and anti-bonding combinations of Bi and Se P_z orbitals, and the parity is a good quantum number at the Γ point due to the spatial inversion symmetry. The topological properties of the Bi_2Se_3 family can be well explained by the band inversion between two sets of Kramer's degenerate states with opposite parity at the Γ point. Here we will show that the band inversion not only gives the non-trivial topological index but also increases the spin susceptibility dramatically. For simplicity, we focus on a 2D sheet in the k-space with $k_z = 0$ (the situation of general k_z is qualitatively similar), where the above effective Hamiltonian reduces to two diagonal blocks as[10,19]

$$H_{2D}(\mathbf{k}) = \begin{bmatrix} h(k) & 0 \\ 0 & h^*(-k) \end{bmatrix} \tag{3}$$

with $h(k) = \mathcal{M}(\mathbf{k})\sigma_z + A_{xy}(k_x\sigma_x + k_y\sigma_y) + \epsilon_0(\mathbf{k})$. The two eigen-states of $h(k)$ give the occupied and unoccupied bands respectively, which can be denoted as $|ck\rangle$and $|vk\rangle$. It is then obvious that the amplitude of the matrix element $\langle ck|\hat{S}_z|vk\rangle$ reaches the maximum value when $\mathcal{M}(\mathbf{k}) = 0$. The above condition can only be satisfied when $M_0 B_{xy} < 0$, which is exactly the condition for the band inversion. In the normal phase without inverted bands, the maximum value of $\langle ck|\hat{S}_z|vk\rangle$ can not be reached and the spin susceptibility is less pronounced compared to the system with band inversion.

To further demonstrate this argument, we perform first-principles calculations (see ref.[33] for method) for the electronic structures and the spin susceptibility of Bi_2Se_3 bulk. The results as function of SOC strength are plotted in Fig. 1(a). When the relative SOC strength

λ/λ_0 is larger than 0.5, the bands at the Γ point are inverted, and the spin susceptibility starts to increase appreciably around this point.

III. MEAN FIELD THEORY FOR THE MAGNETIC TOPOLOGICAL INSULATORS

In the following, we apply a tight binding version of the Zener model[20–22] to calculate the possible Curie temperature at the mean field level. Let's first assume that some magnetic local moments are introduced iso-electronically into the Bi_2Se_3 compounds without changing the insulating behavior. We show that ferromagnetic ordering with T_c as high as 70K can be achieved via the van-Vleck paramagnetism, without requiring the existence of free carriers as in conventional DMS systems. The total Hamiltonian of our system can be written as

$$H_{total} = H_{LDA} + \sum_{I\mu\nu,\alpha=xyz} J_{eff}\mathbf{S}_I^\alpha \cdot \mathbf{s}_{\mu\nu}^\alpha c_{I,\mu}^\dagger c_{I,\nu} + h.c. \tag{4}$$

with

$$H_{LDA} = \sum_{ij,\mu\nu} t_{ij}^{\mu\nu} c_{i,\mu}^\dagger c_{j,\nu}$$

is the single particle Hamiltonian (obtained from first-principles calculations) expressed in the basis of local Wannier functions[33]. Here i and j denote the sites, I only runs over all the unit cells containing magnetic ions and $\mu\nu$ are the orbital/spin indices. The coupling strength between the local spin $\mathbf{S}_I$ and the band spin $\mathbf{s}_{\mu\nu}$ of band electrons is described by the effective exchange parameter J_{eff}.

Performing the mean field approximation and applying the virtual crystal approximation (CPA) to average out the spatial inhomogeneity, Eq.(4) can be written as

$$H_{MF} = H_e + H_L - xJ_{eff}\mathbf{M}_L^\alpha \cdot \mathbf{M}_e^\alpha \tag{5}$$

where $\mathbf{M}_L^\alpha = \langle \mathbf{S}_{I=0}^\alpha \rangle$, $\mathbf{M}_e^\alpha = \left\langle \mathbf{s}_{\mu\nu}^\alpha c_{0,\mu}^\dagger c_{0,\nu} \right\rangle$ are the mean field magnetization for the local moments and band electrons respectively, with

$$H_e = H_{LDA} + \sum_{i\mu\nu}^{\alpha=xyz} J_{eff}\mathbf{M}_L^\alpha \cdot s_{\mu\nu}^\alpha c_{i,\mu}^\dagger c_{i,\nu} + h.c.$$

and

$$H_L = \sum_{I}^{\alpha=xyz} J_{eff}\mathbf{S}_I^\alpha \cdot \mathbf{M}_e^\alpha$$

We choose the concentration of the magnetic ion to be 5%, the total angular momentum of a single magnetic ion to be $J = 3/2$ and the effective exchange coupling $J_{eff} = 2.0eV$, which are in the same order with the quantitative first-principles calculations (as described later). The above mean field equations have been solved self-consistently, and the ordered moment as well as Curie temperature can be calculated. In Fig.1(b), the calculated magnetization versus temperature are plotted for both bulk material and thin film system with 3, 4, 5 quintuple layers (QL) thicknesses. The Curie temperature for the bulk system is around 70K, which can be well compared with previous experimental studies[28–30]. The ferromagnetic ordering is anisotropic, and the Curie transition is of the Ising type, with a finite transition temperature in 2D. Our mean field calculation also indicates that for the thin film system, the Curie temperature is only slightly reduced due to the finite size effect, which give rise to the possible QAHE as discussed below.

IV. ELECTRONIC STRUCTURES OF BI_2SE_3 DOPED WITH TRANSITION METAL ELEMENTS

In this section, we shall show, by parameter-free first principles calculations, that the insulating magnetic ground state discussed above can be indeed obtained by proper choice of magnetic dopants. It has been suggested by experiments[28–30] that the magnetic dopants, such as Ti, V, Cr and Fe, will mostly substitute the Bi ions (or the Sb ions in the case of Sb_2Te_3), we therefore concentrate on this situation in the following discussions. Since the nominal valence of Bi (or Sb) ions are 3+, a general rule is to find a transition metal element which may have a stable 3+ chemical state, so that no free carriers are introduced by this iso-electronic substitution. In addition, due to the coexistence of orbital and spin degrees of freedom of magnetic dopants (due to the partially filled *d*-shells), we need a mechanism to quench these degrees of freedom and stabilize the insulating state. We shall show that such conditions can be satisfied by the combination of crystal field splitting and large Hund's rule coupling for Cr and Fe dopants.

We performed self-consistent first-principle calculations[33] for Bi_2Se_3 doped with various transition metal elements, Ti, V, Cr and Fe. We use a large supercell (of size 3×3×1) with one of the Bi atoms substituted by a magnetic dopant. The crystal structure and the magnetic state are fully optimized to obtain the ground state. The results shown in Fig.2

suggest that a insulating magnetic state is obtained for Cr or Fe doping, while the states are metallic for Ti or V doping cases. To understand the results, we first point out that, for all the cases, the dopants are nearly in the 3+ valence state, and we always obtain the high-spin state due to the large Hund's rule coupling of $3d$ transition metal ions. Thus the charge and spin degrees of freedom are nearly frozen. This will directly lead to the insulating state of Fe-doped samples, because the Fe^{3+} has five $3d$ electrons, favoring the $d^{5\uparrow}d^{0\downarrow}$ configuration in a high-spin state, resulting in a gap between the majority and minority spins. We now consider the orbitals for other dopants. The local environment of dopants, which substitute the Bi sites, is a octahedral formed by six nearest neighboring Se^{2-} ions. Such a local crystal field splits the d-shell into t_{2g} and e_g manifolds. This splitting is large enough to stabilize the $t_{2g}^{3\uparrow}e_g^{0\uparrow}t_{2g}^{0\downarrow}e_g^{0\downarrow}$ configuration of Cr^{3+} ion, resulting in a gap between the t_{2g} and e_g manifolds. For the case of Ti or V doping, even the t_{2g} manifold is partially occupied, leading to the metallic state. It is important to note that, although the local density approximation in the density functional theory may underestimate the electron correlation effects, the inclusion of electron-electron interaction U (such as in LDA+U method) should further enhanced the gap.

The energy gain due to the spin polarization is about 0.9eV/Fe, 1.5eV/Cr, 0.7eV/V and 0.02eV/Ti, respectively, which are very large numbers except for the case of Ti substitution. From the spin splitting of p orbitals of the band electrons, we can estimate the effective exchange coupling J_{eff} between the local moments and the p electrons[34]. The estimated value is around 2.7eV for Cr and 2.8eV for Fe in Bi_2Se_3. This exchange coupling is comparable to that in GaMnAs[20,34].

V. THE QUANTIZED ANOMALOUS HALL EFFECT

Once the ferromagnetically ordered insulating state is achieved with a reasonable T_c, here in this section, we show that QAH effect can be realized for the 2D thin films. In the thick slab geometry, the spatially-separated two pairs of surface states are well defined for the top and bottom surfaces respectively. However, with the reduction of the film thickness, quantum tunneling between the top and bottom surfaces becomes more and more pronounced, giving rise to finite mass term in the effective 2D model[19]. In the basis of $|+\uparrow\rangle$,$|-\downarrow\rangle$,$|+\downarrow\rangle$,$|-\uparrow\rangle$, with $\pm$ referring to the bonding and anti-bonding combinations

of the top and bottom surface states, and $\downarrow\uparrow$ indicating the spin, the low energy effective model for the thin film can be written in the form of H_{2D} as in Eq. 3, with $h(k) = \Delta_k\sigma_z + v_F\left(k_x\sigma_y - k_y\sigma_x\right)$, $\Delta_k = \Delta_0 + Bk_\parallel^2$, similar to the Bernevig-Hughes-Zhang model describing the low energy physics in HgTe/CdTe quantum well[10]. When $\Delta_0 B < 0$, band inversion occurs, and the system will be in the QSH phase if this is the only band inversion between two subbands with opposite parity, which is exactly the situation in HgTe/CdTe quantum well system. The situation for Bi_2Se_3 film is somewhat different in the sense that more pairs of subbands can get inverted at the Γ point, and the system may still remain in the topologically trivial state if the band inversion occurs even number of times[19]. Nevertheless, as we shall show below, regardless of whether the 4-bands system is originally in the topologically non-trivial phase or not, a strong enough exchange field will induce QAH effect in this system.

The exchange coupling term induced by the finite magnetization in the FM phase can be written as,

$$H_{exchange} = \begin{bmatrix} g_{eff}M\sigma_z & 0 \\ 0 & -g_{eff}M\sigma_z \end{bmatrix} \tag{6}$$

with M denoting the strength of the exchange field and g_{eff} being the effective g-factor of the surface states. Added to the 2D model (3), the exchange field increases the mass term of the upper block and reduces it for the lower block, breaking the time reversal symmetry. More importantly, a sufficiently large exchange field can change the Chern number of one of the two blocks. As schematically illustrated in Fig.3, if the 4-band system is originally in the topologically trivial phase, the exchange field will induce a band inversion in the upper block and push the two sub-bands in the lower block even farther away from each other. Therefore the 2D model with a negative mass in the upper block contributes e^2/h for the Hall conductance. On the other hand, if the system is originally in the topologically non-trivial phase, both blocks have inverted band structures. In this case, a sufficiently large exchange field can increase the band inversion in the upper block and revert the band inversion in the lower block. Again the negative mass in the upper block contributes e^2/h for the Hall conductance. These two scenarios are illustrated in Fig.3.

To be realistic, we carried out quantitative calculations for Bi_2Se_3 films, based on the density functional theory and linear response formalism[33]. A spacial uniform exchange field is included to take into account the effect of magnetization in the FM state at the mean

field level. In Fig.4(a), (b) and (c), we plot the lowest four sub-band levels at Γ point as a function of exchange field. The level crossings (indicated by arrows) between the lowest conduction bands (blue lines) and valence bands (red lines) are found in all the three Bi_2Se_3 thin film systems with different layer thickness. The corresponding Hall conductance can be obtained using the following Kubo formula[3],

$$\sigma_{xy} = e^2\hbar \sum_{nmk} \frac{Im\left[\langle nk|\,\hat{v}_x\,|mk\rangle\,\langle mk|\,\hat{v}_y\,|nk\rangle\right]}{\left(E_{nk}-E_{mk}\right)^2}\left(n_f(E_{nk})-n_f(E_{mk})\right) \tag{7}$$

with E_{nk} being the dispersion of the quantum well sub-bands and $\hat{v}_{x/y}$ being the velocity operators. In the insulator case, where the chemical potential is located inside the energy gap between conduction and valence sub-bands, the Hall conductance is determined by the first Chern number of the occupied bands and must be an exact integer in the unit of e^2/h. The calculated Hall conductance for Bi_2Se_3 thin film with three typical thickness are plotted in figure 4 (d) as function of exchange field, where a jump from "0" to "1" in the Hall conductance are observed at the corresponding critical exchange field for the level crossing.

In Fig.5, we plot the sub-band dispersion and corresponding Hall conductance as function of chemical potential for 3 and 5 QL Bi_2Se_3 thin films with different exchange fields. We can find that the change induced by the exchange field is mainly in the area near Γ point. For the QAH phases ((d) and (h)), non-zero integer plateau is observed when the chemical potential falls into the energy gap. The difference between the 3 and 5 QL cases suggests that the QAH plateau is much narrower for thick film due to the narrower energy gap coming from the intersection of top and bottom surface states.

In conclusion we have shown that magnetic dopants Cr and Fe form long range magnetic order in the insulating state of the Bi_2Se_3 family of topological insulators. The ferromagnetic order lead to a topologically non-trivial electronic structure with quantized Hall conductance without any external magnetic field. In real samples, a small amount of bulk carriers could always be present, however, if the concentration is low enough, they will be localized by disorder in two dimensions, and will not affect the precise quantization of the Hall plateau. The edge states of our QAH state conducts charge current without any dissipation in the absence of any external magnetic field. This effect could enable a new generation of low power electronic devices.

Acknowledgments

We acknowledge the valuable discussions with C. X. Liu, X. L. Qi, Q. Niu, S. Q. Shen, and the supports from the NSF of China, the 973 Program of China (No. 2007CB925000 and 2010CB923000), and the International Science and Technology Cooperation Program of China. SCZ is supported by the US NSF under grant numbers DMR-0904264.

---

[1] E. H. Hall, Philosophical Magazine Series 5 **10**, 301 (1880).

[2] E. H. Hall, Philosophical Magazine Series 5 **12**, 157 (1881).

[3] N. Nagaosa, J. Sinova, S. Onoda, A. H. MacDonald, and N. P. Ong, arXiv:cond-mat/0904.4154 (Accepted by Rev. Mod. Phys.). (2009).

[4] T. Jungwirth, Q. Niu, and A. H. MacDonald, Phys. Rev. Lett. **88**, 207208 (2002).

[5] Z. Fang, N. Nagaosa, K. S. Takahashi, A. Asamitsu, R. Mathieu, T. Ogasawara, H. Yamada, M. Kawasaki, Y. Tokura, and K. Terakura, Science **302**, 92 (2003).

[6] Y. Yao, L. Kleinman, A. H. MacDonald, J. Sinova, T. Jungwirth, D.-s. Wang, E. Wang, and Q. Niu, Phys. Rev. Lett. **92**, 037204 (2004).

[7] K. von Klitzing, G. Dorda, M. Pepper, Phys. Rev. Lett. **45**, 494-497 (1980).

[8] S. Murakami, N. Nagaosa, and S.-C. Zhang, Science **301**, 1348 (2003), 10.1126/science.1087128.

[9] J. Sinova, D. Culcer, Q. Niu, N. A. Sinitsyn, T. Jungwirth, and A. H. MacDonald, Phys. Rev. Lett. **92**, 126603 (2004).

[10] B. A. Bernevig, T. L. Hughes, and S.-C. Zhang, Science **314**, 1757 (2006), 10.1126/science.1133734.

[11] M. König, S. Wiedmann, C. Brüne, A. Roth, H. Buhmann, L. Molenkamp, X.-L. Qi, and S.-C. Zhang, Science **318**, 766 (2007).

[12] X.-L. Qi, Y.-S. Wu, and S.-C. Zhang, Phys. Rev. B **74**, 085308 (2006).

[13] F. D. M. Haldane, Phys. Rev. Lett. **61**, 2015 (1988).

[14] M. Onoda and N. Nagaosa, Phys. Rev. Lett. **90**, 206601 (2003).

[15] C.-X. Liu, X.-L. Qi, X. Dai, Z. Fang, and S.-C. Zhang, Phys. Rev. Lett. **101**, 146802 (2008).

[16] H. Zhang, C.-X. Liu, X.-L. Qi, X. Dai, Z. Fang, and S.-C. Zhang, Nature Phys. **5**, 438 (2009), 10.1038/nphys1270.

[17] Y. Xia, D. Qian, D. Hsieh, L. Wray, A. Pal, H. Lin, A. Bansil, D. Grauer, Y. S. Hor, R. J. Cava *et al.*, Nature Phys. **5**, 398 (2009), 10.1038/nphys1274.

[18] Y. L. Chen, J. G. Analytis, J. H. Chu, Z. K. Liu, S. K. Mo, X. L. Qi, H. J. Zhang, D. H. Lu, X. Dai, Z. Fang *et al.*, Science **325**, 178 (2009).

[19] C.-X. Liu, H. Zhang, B. Yan, X.-L. Qi, T. Frauenheim, X. Dai, Z. Fang, and S.-C. Zhang, arXiv.org:0908.3654 (accepted by Phys. Rev. B, 2010 in press).

[20] T. Jungwirth, J. Sinova, J. Mašek, J. Kučera, and A. H. MacDonald, Rev. Mod. Phys. **78**, 809 (2006).

[21] T. Dietl, H. Ohno, F. Matsukura, J. Cibert, and D. Ferrand, Science **287**, 1019 (2000).

[22] T. Dietl, H. Ohno, and F. Matsukura, Phys. Rev. B **63**, 195205 (2001)

[23] H. Ohno, Science **281**, 951 (1998).

[24] G. Zhang, H. Qin, J. Teng, J. Guo, Q. Guo, X. Dai, Z. Fang, and K. Wu, Applied Physics Letters **95**, 053114 (pages 3) (2009).

[25] Y.-Y. Li, G. Wang, X.-G. Zhu, M.-H. Liu, C. Ye, X. Chen, Y.-Y. Wang, K. He, L.-L. Wang, X.-C. Ma *et al.*, arXiv.org:0912.5054 (2009).

[26] Y. Zhang, K. He, C.-Z. Chang, C.-L. Song, L. Wang, X. Chen, J. Jia, Z. Fang, X. Dai, W.-Y. Shan *et al.*, arXiv.org:0911.3706 (2009).

[27] T. Zhang, P. Cheng, X. Chen, J.-F. Jia, X. Ma, K. He, L. Wang, H. Zhang, X. Dai, Z. Fang *et al.*, Phys. Rev. Lett. **103**, 266803 (2009).

[28] V. Kul bachinskii, A. Kaminskii, K. Kindo, Y. Narumi, K. Suga, P. Lostak, and P. Svanda, JETP Letters **73**, 352 (2001), 10.1134/1.1378118.

[29] J. S. Dyck, P. Hájek, P. Lošt'ák, and C. Uher, Phys. Rev. B **65**, 115212 (2002).

[30] Y. J. Chien, *Transition Metal-Doped* Sb_2Te_3 *and* Bi_2Te_3 *Diluted Magnetic Semiconductors*, Ph.D dissertation, University of Michigan, USA (2007).

[31] J. H. Van Vleck, The Theory of Electronic and Magnetic Susceptibilities (Oxford University Press, London, 1932).

[32] The parameters in Eq.(2) are determined by fitting to the *ab initio* results[16], which gives M_0=-0.28eV, A_{xy}=2.2eVÅ, A_z=4.1eVÅ, B_{xy}=10eVÅ^2, B_z=56.6eVÅ^2, C=-0.0068eV, D_{xy}=1.3eVÅ^2, D_z=19.6eVÅ^2.

[33] The plane wave pseudopotential calculations were done using the BSTATE package in the framework of the Perdew-Burke-Ernzerhof-type (PBE-type) generalized gradient approxima-

tion (GGA) of the density functional theory. The spin-orbit coupling is included from pseudopotentials, and the convergence with respect to cutoff energy and K-points sampling are well checked. From the calculated Bloch eigen functions of ground state, maximally localized Wannier functions can be constructed[16]. Such Wannier functions are used to construct the low energy effective Hamiltonian H_{LDA} for free-standing slab of Bi_2Se_3 film. Adding proper Zeeman term into effective Hamiltonian, ferromagnetic ordering and QAH effects are studied without free parameters.

[34] S. Sanvito, G. Theurich, and N.A. Hill, J. Supercond. **15**, 85 (2002).

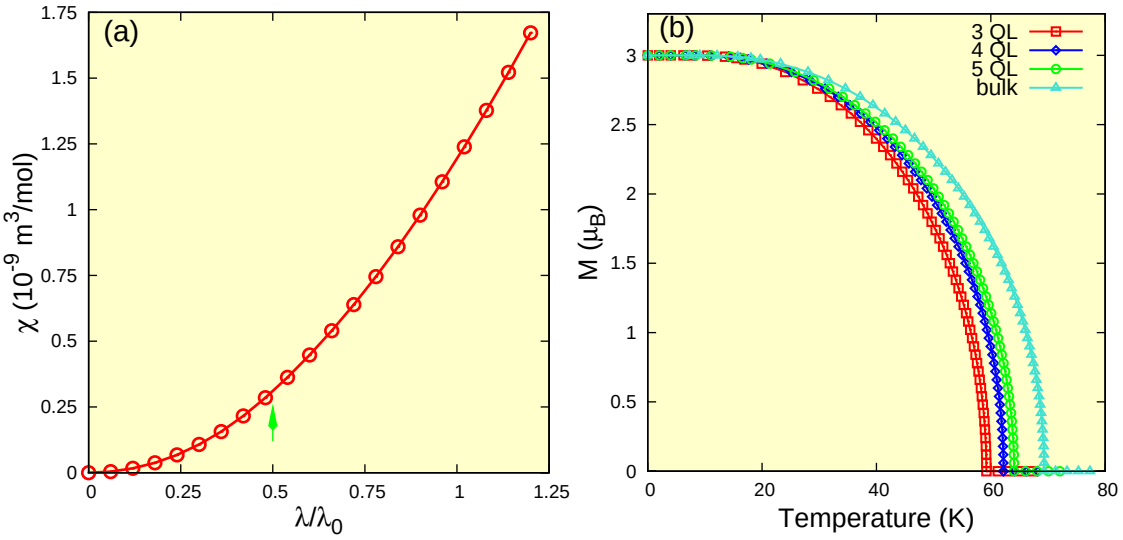

FIG. 1: **The calculated spin susceptibility and Curie temperature for Bi_2Se_3.** (a) The Van-Vleck type spin susceptibility of Bi_2Se_3 bulk as a function of spin-orbital-coupling (SOC) strength. λ_0 is the real SOC strength, and it is uniformly scaled to simulate various SOC strength λ. When λ/λ_0 is larger than 0.5, the energy bands at Γ are inverted, and Bi_2Se_3 becomes strong topological insulator. (b) The spontaneous magnetization M as a function of temperature for Cr-doped (S_z=3/2) Bi_2Se_3 bulk as well as thin films with thickness of 3, 4 and 5 quintuple layers (QL).

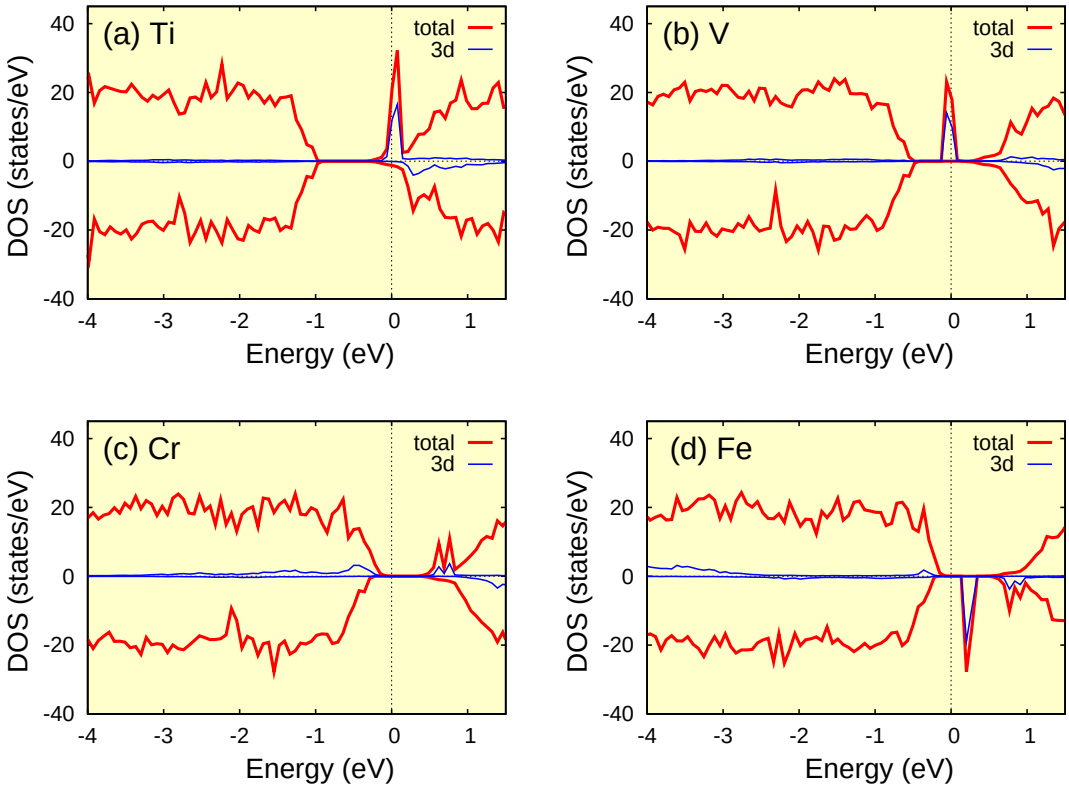

FIG. 2: **The calculated density of states (DOS) for Bi_2Se_3 doped with different transition metal elements**. The Fermi level is located at energy zero, and the positive and negative values of DOS are used for up and down spin, respectively. The blue lines are projected partial DOS of the $3d$ states of transition metal ions. It is shown that Cr or Fe doping will give the insulating magnetic state.

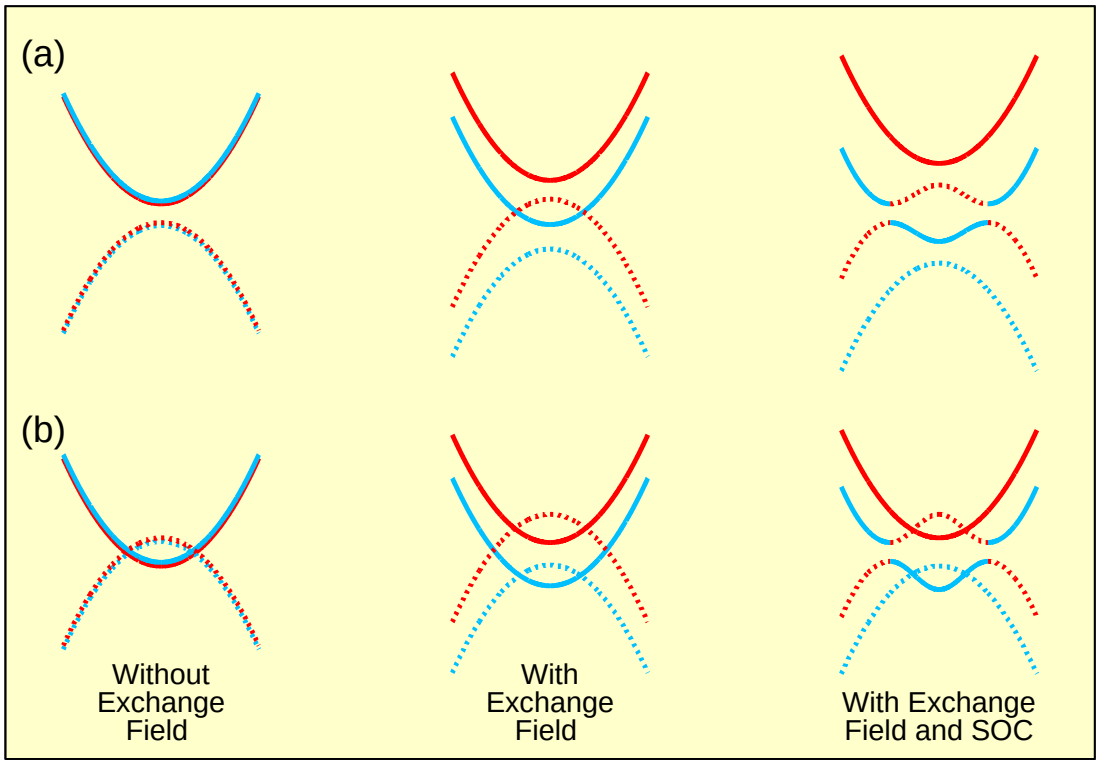

FIG. 3: **Evolution of the sub-bands structure upon increasing the exchange field.** The solid (dashed) lines denote the sub-band which have even (odd) parity at Γ point, and the blue (red) color denotes the spin down (up) electrons. (a) The initial sub-bands are not inverted. When a exchange field is introduced, the spin down sub-bands (blue lines) are pushed down and the spin up sub-bands (red lines) are lifted up. When the exchange field is strong enough, a pair of inverted sub-bands appear (the red dash line and the blue solid line). (b) The initial sub-bands are already inverted at Γ point. The exchange field reverts the band inversion in one pair of sub-bands (the red solid line and the blue dashed line) and increase the band inversion in the other pair of sub-bands (the red dash line and the blue solid line). The SOC opens a gap at the cross points of spin-up and spin-down subbands as shown on the right most panel of (a) and (b), leading to the QAH state by the mechanism proposed in Ref.[12,15]

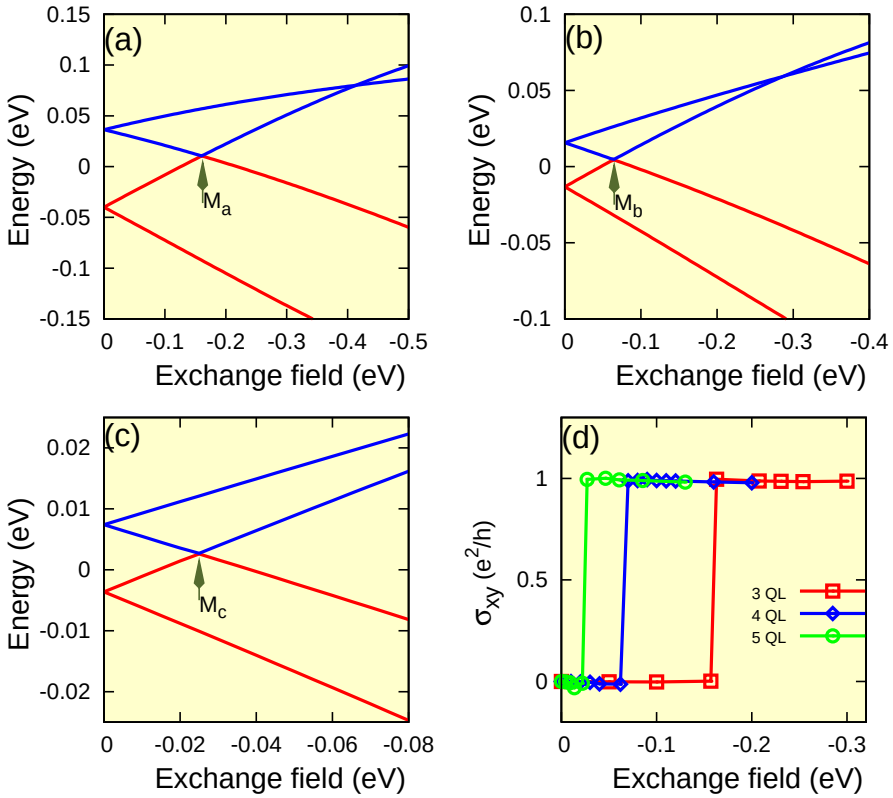

FIG. 4: **The quantized anomalous Hall(QAH) conductance.** (a), (b) and (c) are the lowest sub-bands at the Γ point plotted versus the exchange field, for Bi_2Se_3 films with thickness of 3, 4 and 5QL, respectively. The red (blue) lines denote the occupied (unoccupied) states. With the increasing of the exchange field, a switch of occupied and unoccupied states happens (i.e, a quantum phase transition to the QAH phase) at the critical field strength indicated by arrows. (d), The calculated Hall conductance using the Hamiltonian from first-principles calculations under an uniform exchange field (see text for the detail) for 3, 4 and 5QL Bi_2Se_3 films. As we expect, the Hall conductance is zero before the QAH transition, but $\sigma_{xy} = e^2/h$ afterwards.

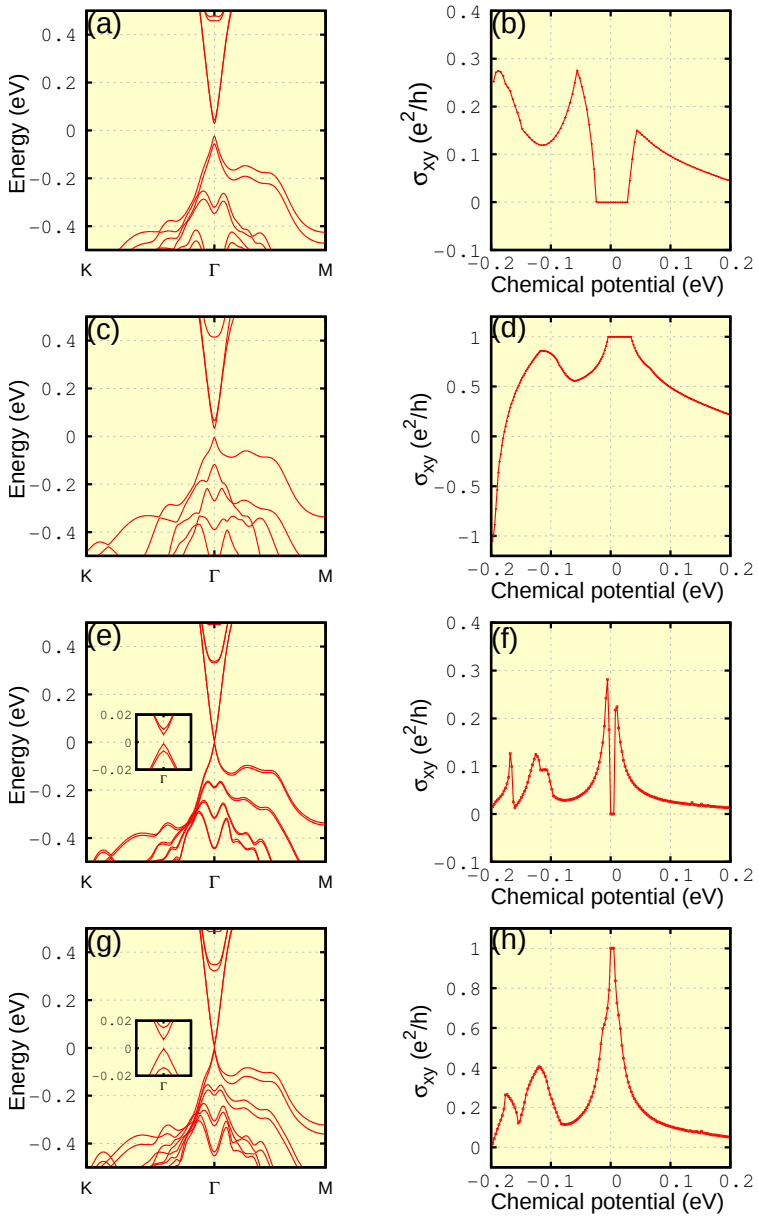

FIG. 5: **The sub-bands dispersion and the Hall conductance.** The sub-bands dispersion of 2D Bi_2Se_3 thin film are plotted for (a) 3QL slab at exchange field=-0.05eV, (c) 3QL slab at exchange field=-0.24eV, (e) 5QL slab at exchange field=-0.01eV, and (g) 5QL slab at exchange field=-0.04eV. The insets of (e) and (g) zoom out the dispersion near Γ point. The corresponding Hall conductance are plotted in the right panels ((b), (d), (f) and (g)) as the function of the chemical potential. The systems in (a) and (e) are normal insulators, which have zero platforms in Hall conductance when the chemical potential locates in the energy gap. The system in (c) and (g) are QAH insulators, in which the Hall conductance have quantized value: e^2/h.